Available online at www.sciencedirect.com

ScienceDirect

Procedia Chemistry 3 (2011) 211–221

Chemistry Procedia

22nd Solvay Conference on Chemistry

Electronic coherence effects in photosynthetic light harvesting

Tzu-Chi Yen[a], Yuan-Chung Cheng[a*]

[a]*Department of Chemistry and Center for Quantum Science and Engineering, National Taiwan Univesity, Taipei, Taiwan*

Abstract

Photosynthetic light harvesting is a paradigmatic example for quantum effects in biology. In this work, we review studies on quantum coherence effects in the LH2 antenna complex from purple bacteria to demonstrate how quantum mechanical rules play important roles in the speedup of excitation energy transfer, the stabilization of electronic excitations, and the robustness of light harvesting in photosynthesis. Subsequently, we present our recent theoretical studies on exciton dynamical localization and excitonic coherence generation in photosynthetic systems. We apply a variational-polaron approach to investigate decoherence of exciton states induced by dynamical fluctuations due to system-environment interactions. The results indicate that the dynamical localization of photoexcitations in photosynthetic complexes is significant and imperative for a complete understanding of coherence and excitation dynamics in photosynthesis. Moreover, we use a simple model to investigate quantum coherence effects in intercomplex excitation energy transfer in natural photosynthesis, with a focus on the likelihoods of generating excitonic coherences during the process. Our model simulations reveal that excitonic coherence between acceptor exciton states and transient nonlocal quantum correlation between distant pairs of chromophores can be generated through intercomplex energy transfer. Finally, we discuss the implications of these theoretical works and important open questions that remain to be answered.

Keywords: Photosynthesis; Light Harvesting; Exciton; Quantum Coherence; Exciton Dynamical Localization

1. Introduction

Highly efficient energy harvesting and trapping performed by photosynthetic systems are critical to the success of photosynthesis [1-3]. Photosynthetic light harvesting involves the absorption of sunlight by pigments in the antenna complexes of a photosynthetic unit, and the subsequent transfer of the excitation energy across multiple pigments and light-harvesting complexes to the reaction center. Remarkably, this process exhibits a quantum efficiency of > 95% for most photosynthetic organisms at low-light conditions. Understanding the rapid excitation energy transfer (EET) process in photosynthesis requires an explicit quantum mechanical description [4]. It is therefore fitting that this work, being a contribution in the "quantum effects in biology" section of the 22nd Solvay Conference on Chemistry, shall be focused on the quantum coherence effects in photosynthetic light harvesting.

The nanoscale dimensions of photosynthetic complexes result in strong couplings between chromophores, which give rise to delocalized exciton states and coherent, wavelike propagation of excitation energy in space. Recent experimental [5-9] and theoretical [10-14] investigations into the mechanisms of EET in photosynthetic complexes

* Corresponding author. Tel.: +886-2-33669788; fax: +886-2-23636359.
E-mail address: yuanchung@ntu.edu.tw.

1876–6196 © 2011 Published by Elsevier Ltd. Selection and/or peer-review under responsibility of G.R. Fleming, G.D. Scholes and A. De Wit
doi:10.1016/j.proche.2011.08.028

have indicated that quantum coherence effects contribute to the tuning and optimization of the efficiency of photosynthetic light harvesting. However, the generality of quantum coherence in photosynthetic systems, the significance of quantum aspects in the biological functions of photosynthetic light harvesting, and the physical mechanisms that are responsible for remarkable efficiency remain largely unclear.

How does quantum coherence influence the energetics and mechanism of photosynthetic light harvesting? How does temperature and environmental fluctuations affect coherence of photosynthetic excitations? What is the significance of coherence beyond photoexcitation by coherent laser pulses? We aim to address these questions in this work. In Sec. 2, we provide the theoretical background by describing the model for photosynthetic EET and give explicit definitions of two types of coherence effects. We then briefly review coherence effects and the clear benefits of coherence in the LH2 complex of purple bacteria in Sec. 3, which we consider as a primary example for quantum effects in light harvesting. In Sec. 4 and Sec. 5, we then present two theoretical studies that addressed two largely overlooked phenomena in the discussions of EET dynamics in light harvesting. We applied a variational-polaron approach to study the dynamical localization effects in a model dimer system and demonstrate that the renormalization of effective electronic coupling by electron-phonon couplings lead to complex EET dynamics and non-trivial coherence effects (Sec. 4). Finally, we examine a simple trimer system in Sec. 5 to investigate the coherence effects in intercomplex transfer. We show that, in contrast to conventional Förster picture of EET, excitonic coherence can be generated in intercomplex transfers and even when couplings are small, long-range coherence between distant chromophores can be generated.

Nomenclature

EET	excitation energy transfer
BChl	bacteriochlorophyll
MC-FRET	multichromophoric Förster resonance energy transfer theory
FMO	the Fenna-Matthews-Olson protein of green sulfur bacteria
LH2	the LH2 antenna complex of purple bacteria

2. Photosynthetic Exciton and Quantum Coherence

To describe photoexcitations of a photosynthetic pigment-protein complex, we consider a system of *N* pigments described by the following Frenkel exciton Hamiltonian:

$$H_e = \sum_{n=1}^{N} \varepsilon_n |n\rangle\langle n| + \sum_{n \neq m} J_{nm} |n\rangle\langle m|, \tag{1}$$

where $|n\rangle$ denotes an excited state localized at site n, ε_n is the site excitation energy of $|n\rangle$, and J_{nm} is the excitonic coupling between $|n\rangle$ and $|m\rangle$. In addition, a reasonable model for photosynthetic excitations should include static energy disorder that modulates the site energies, $\varepsilon_n = \varepsilon_n^{(0)} + \delta\varepsilon_n$, where $\delta\varepsilon_n$ are random variables that are often treated by Monte Carlo sampling over a Gaussian distribution.

Equation (1) represents the Hamiltonian in a basis of localized molecular excitations (site basis), which is an appropriate representation when the excitonic couplings are small relative to the site energy gaps or the width of energetic disorder. When excitonic couplings are significant, it is more appropriate to consider the problem in the basis of the eigenstates of H_e, the so-called exciton states. Exciton states in a photosynthetic complex are usually linear combinations of molecular excitations and delocalized over several chromophores, and they form the basis for the description of optical properties and EET dynamics of light harvesting.

In addition to H_e, the environment (bath) that modulates the electronic excitations and causes relaxation has to be included in a model for EET. Typically, the bath is modeled as a harmonic phonon bath so that the total exciton-plus-phonon Hamiltonian is [1,3,4,15]

$$H_{TOT} = H_e + H_{ph} + H_{e-ph}, \tag{2}$$

where the electron-phonon (e-ph) coupling Hamiltonian is usually taken as diagonal in site basis and linear in phonon coordinates:

$$H_{e-ph} = \sum_{n=1}^{N} \sum_i g_{n,i}\omega_i |n\rangle\langle n| \left(b_i + b_i^\dagger\right), \tag{3}$$

where b_i (b_i^+) is phonon annihilation (creation) operator, ω_i denotes phonon frequency, and $g_{n,i}$ denotes e-ph coupling constant. This form of $H_{e\text{-}ph}$ represents phonon-induced fluctuations of the site energies on each chromophore. Regarding the dyamics of EET, the details of the bath are not important and can be treated statistically using the spectral density, $J_n(\omega)$, which represents the density of states and coupling strengths of the phonon bath coupled to the *n*-th chromophore. In principle, the spectral density can be estimated from ultrafast time-resolved experiments [16]. This microscopic model provides the basis to calculate the EET dynamics through perturbative treatments [4,15] or nonperturbative means [17,18].

With the theoretical background covered, we are now ready to come back to the main subject of this Solvay conference. The main quantum aspects in photosynthetic light harvesting are often coarsely referred to as "coherence", which by definition is an off-diagonal density matrix element that is indicative of superposition states of the chosen basis. Since a basis that diagonalizes the density matrix can always be applied to remove all coherences, this definition is ambiguous. In fact, two types of coherences can be identified in the literature. The first one is the site coherence between two chromophores, manifested in delocalized exciton states. The second type of coherence in light harvesting alludes to the coherent wave-like dynamics of EET [6-9, 12], which actually reflects a superposition of excitons. Note that the site basis and the exciton basis are special because they are related to the spatial arrangement of chromophores and energy eigenstates of the Hamiltonian, respectively. It is necessary to differentiate coherences in these two distinct basis sets, because they correspond to different quantum effects in light harvesting. In this work we use coherence to refer to site coherence, and explicitly use excitonic coherence for the second type. As will be shown in the next section, both types of coherence effects play important roles in photosynthetic light harvesting.

3. Coherence Effects in the LH2 Antenna Complex of Purple Bacteria

The LH2 antenna complex of purple bacteria provides an excellent example that displays quantum coherence effects in photosynthetic light harvesting. The X-ray crystal structures of the LH2 complex revealed remarkable symmetry in the arrangement of bacteriochlorophylls (BChls). For example, the LH2 complex of *Rps. acidophila* consists of 27 BChl a molecules arranged into two highly symmetric rings; 9 of them form the so called B800 ring which absorbs maximally at 800 nm, and the other 18 form the B850 ring which absorbs maximally at 850 nm. In Fig. 1(a), we show the geometrical arrangement of the 27 BChl a molecules. The Mg-Mg distance between adjacent B800 BChl a molecules is 21 Å, which results in the weak nearest-neighbor electronic couplings (~ -25 cm^{-1}) in the B800 ring [19]. The Mg-Mg distance between BChl a pigments in the B850 ring is ~ 9.6 Å, leading to strong nearest-neighbor coupling of ~ -300 cm^{-1} in the B850 ring [20]. Because of the strong electronic coupling between BChls [21-23], a delocalized exciton description is required for B850 excited states.

Quantum coherence in the B850 ring of the LH2 complex plays a crucial role in its light harvesting, energy storage, and rapid EET dynamics [23-26]. Figure 1(b) shows the energy levels of the B850 excitons and the absorption spectrum of the LH2 complex. Due to the delocalized nature of the B850 excitons and the circular arrangement of the transition dipoles of the B850 BChls, the optical oscillator strength is concentrated on the k=±1 states that are responsible for the B850 band in the absorption spectrum. In addition, strong excitonic couplings between B850 BChls allow the energy levels of the B850 states to span a broad spectral range with dark states close in energy to the B800 manifold, enabling efficient EET from the B800 system to the B850 ring. In addition to energy tuning, coherence also plays a crucial role in the B800→B850 EET. Jang, Newton and Silbey have demonstrated that using the simple Förster theory, which neglects coherence between B850 BChls, underestimates the B800→B850 rate by an order of magnitude, while the explicit treatment of B850 coherence in their

multichromophoric Förster resonance energy transfer theory (MC-FRET) yields results in good agreement with experiments [26]. Moreover, strong couplings in the B850 system allow rapid energy relaxation into the k=0 state, which is a dark state with small oscillator strength that can minimize the loss due to fluorescence deexcitation.

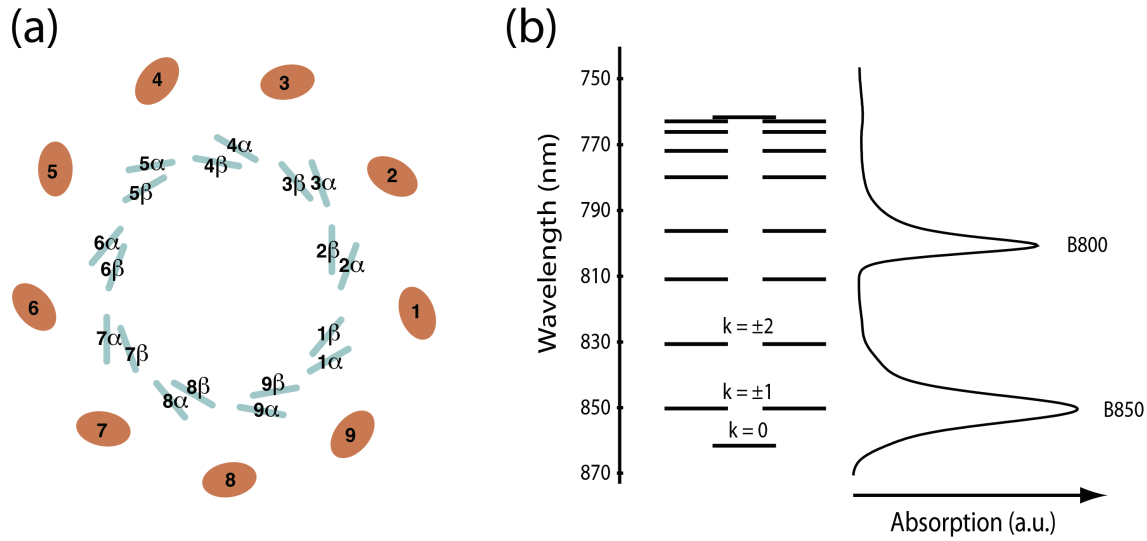

Fig.1. (a) A graphical illustration showing the arrangement of bacteriochlorophylls in the LH2 complex of *Rps. acidophila*. The outer ring represents the B800 unit, and the inner ring represents the B850 unit. (b) The energy levels of the B850 excitons and the absorption spectrum of the LH2 complex at 6K. The B850 energies are taken from a recent calculation in Ref. [27].

An even subtler coherence effect occurs in the B800 ring. Typically, the B800 excitations are considered to localize on individual pigments because the excitonic couplings between B800 BChls are smaller than the energetic disorder in the system [28,29]. However, a detailed investigation of the low-temperature spectrum of the B800 band revealed that coherence in the B800 ring subtly changes both the spectrum and EET dynamics in the LH2 complex [30]. Figure 2(a) shows the simulated density of states and the spectral lineshape for an ensemble of B800 rings. While the density of states is a symmetric function, the spectral lineshape is asymmetric, with a pronounced tail in the blue side of the band. In Fig.2(b), we compare the simulated spectrum to the low-temperature B800-only ensemble spectrum. The excellent agreement indicates that although the B800 lineshape is dominated by inhomogeneous line broadening, the effect of coherence exists and results in the blue tail. The asymmetric lineshape is due to the redistribution of dipole moments in the B800 band (Fig.2(c)), because the B800 excitations are coherently delocalized on multiple BChls. Figure 2(d) shows the participation ratio for the B800 exciton states as a function of the exciton excitation energy. Note that the inverse of the participation ratio is a measure of the delocalization length. Therefore, Figure 2(d) indicates that a majority of the B800 states are delocalized on 2-4 pigments. The calculation clearly shows that the coherence in the B800 ring cannot be neglected, and the blue tail in the ensemble spectrum presents a signature of the quantum coherence.

The quantum coherence in the B800 ring also influences the dynamics of the B800→B850 EET. Since the average participation ratio is close to 0.5 in a wide regime of the B800 band (Fig.2(d)), a reasonable model for the B800 excited state is a coherent exciton delocalized on a nearest-neighbor dimer. As a result, coherence allows rapid intraband transfer between B800 BChls to provide alternative EET pathways when a direct transfer to the B850 is slow. Simulations indicate that the B800 coherence makes the B800→B850 EET rate more uniform and hence more robust against energetic disorder in the system [30]. Moreover, Jang, Newton and Silbey calculated B800→B850 EET rates at varying bias of the average excitation energy of the B800-BChl relative to that of the B850-BChl. They discovered that coherence in the multichromophoric aggregate of the B850 ring provides subtle energetic optimization that keeps EET rates stable against energetic disorder [31]. In summary, delocalized exciton states in

the LH2 complex play crucial roles in the EET dynamics of the system, and are also tightly related to the design and optimization of the light-harvesting complex. These coherence-assisting principles will have to be tested in other photosynthetic complexes to see if they are general. Interestingly, recent work by Schlau-Cohen *et al.* also indicates the importance of coherence in defining the pathways of energy flow in the LHCII complex of higher plants [32].

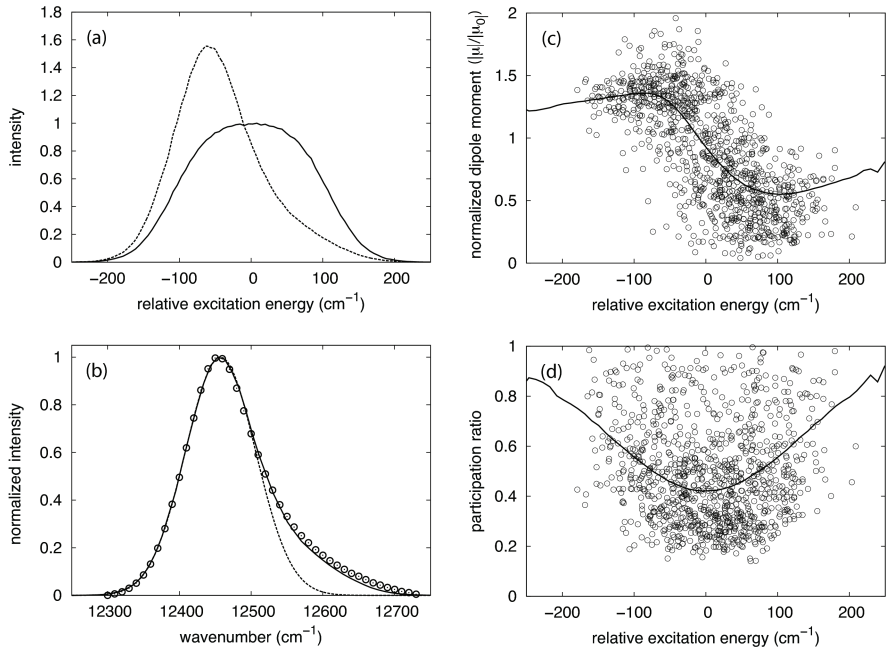

Fig.2. Simulation results for an ensemble of the B800 rings from *Rps. acidophila* including static disorder and quantum coherence effect (Ref. [30]) (a) The simulated density of states (solid line) and the inhomogeneous spectral lineshape (dashed line). (b) A comparison of the simulated spectrum (solid line) with the ensemble absorption spectrum (open circle). A Gaussian fit to the red side of the simulated spectrum (dashed line) is also presented to show that the long tail at the blue side of the band cannot be explained by a Gaussian inhomogeneous lineshape. (c) Scatter plot of participation ratio and (d) amplitude of dipole moment as a function of excitation energy for exciton states in the B800 ring. The solid lines are average values as a function of the excitation energies. For details, see Ref. [30].

The excitonic coherence effect that produces coherent wavelike EET also plays an important role in the dynamics of the LH2 complex, particularly in the strongly coupled B850 ring. Kuhn *et al.* [33] investigated the fluorescence anisotropy decay for the B850 band of the LH2 antenna complex of the purple bacterium *Rps. acidophila* and showed that nonsecular terms in the Redfield tensor, which include coherence transfer and population to coherence transfer terms, improve the calculated time scales for polarization decay in comparison with the experiment. Moreover, by carefully comparing emission spectral dynamics of single LH2 complexes and theoretical simulations, Novoderezhkin *et al.* demonstrated that intraring EET in the B850 system can proceed via a coherent wavelike motion [34]. In addition, Novoderezhkin *et al.* studied the anisotropy decay in the B800 band of the antenna LH2 complex from *Rh. molischianum*, and found that the experimental data at short times (0-2 ps) require a description based on the full Redfield treatment in order to reproduce long-lived coherences and higher anisotropy values observed in the experiment [35]. These studies clearly demonstrated that the excitonic coherence, i.e. reversible wavelike dynamics, are important in the energy relaxation in the LH2 antenna complex [5].

In conclusion, coherence is fundamental to the function of the LH2 complex. In the following sections, we examine two important yet mostly overlooked aspects of quantum coherence. First, analysis of photosynthetic coherence effects in the literature almost always adopted a model of temperature-independent electronic couplings, neglecting the effects of dynamical localization. Because dynamical fluctuations can destroy coherence and localize exciton states, an understanding of the dynamical localization effects is essential for the evaluation of coherence contribution to the EET dynamics. This is particularly important when considering temperature-dependent effects. Second, the excitonic coherence effects observed in laser-induced dynamics in the B850 ring of the LH2 cannot be

taken for granted. What is their significance in natural photosynthesis, in which B800 to B850 transfer is important? The MC-FRET picture of energy transfer considers energy transfer between eigenstates and therefore does not induce excitonic coherence in the B850 ring. This leads to the prediction that excitonic coherence is not important in the subsequent B850 intra-ring dynamics. Does this picture provide satisfactory description? In the next two sections, we will discuss these two important issues that are highly relevant in the elucidation of quantum effects in photosynthesis.

4. Dynamical Localization

The description of quantum coherence and electronic coupling presented in Sec. 2 is based on constant mean-field electronic couplings. In this picture, electronic eigenstates are independent of temperature and strength of e-ph couplings. However, at high temperatures or large e-ph couplings, dynamical fluctuations could destroy coherence between pigments, leading to dynamical localization. Therefore, the effective electronic coupling, hence the effective delocalization length, should be a function of temperature as well as the strength of e-ph couplings. These exciton self-trapping physics for excitations in a polarizable medium was first introduced by Landau, and later fully developed by Rashba and Toyozawa [36, 37]. To investigate the effects of dynamical localization, we must go beyond the conventional Redfield theory and Förster theory of EET and adopt a theoretical formalism that determines the zeroth-order description based on physical parameters. Here, we apply a variational method to investigate the effects of dynamical localization. A similar approach was originally developed by Yarkony and Silbey for exciton transport in molecular crystals [38] and later adopted by Silbey and Harris to treat tunneling in a spin-boson model [39, 40]. More recently, Cheng and Silbey have extended the method to successfully describe the temperature-dependent coherent to incoherent transport transition in molecular crystals of polyacenes [41].

Consider the following unitary transformation that represents site-dependent displacement of phonon coordinates:

$$U = \exp\left\{-f_0 \sum_{n,i} g_{n,i} |n\rangle\langle n| \left(b_i - b_i^\dagger\right)\right\} \tag{4}$$

where f_0 is a *dressing factor* that ranges from 0 to 1 and will be determined variationally. Apply the unitary transformation to the exciton-phonon Hamiltonian, we obtain in the dressed basis:

$$\begin{aligned}\tilde{H}_{TOT} &= U H_{TOT} U^\dagger \\ &= \sum_{n,i}\left[\varepsilon_n + (f_0^2 - 2f_0) g_{n,i}^2 \omega_i\right] |n\rangle\langle n| + \sum_{n\neq m} J_{nm} \left\langle \theta_n^\dagger \theta_m \right\rangle |n\rangle\langle m| \\ &\quad + H_{ph} + (1-f_0)\sum_{n,i} g_{n,i}\omega_i |n\rangle\langle n| (b_i^\dagger + b_i) + \sum_{n\neq m} J_{nm}\left(\theta_n^\dagger \theta_m - \left\langle \theta_n^\dagger \theta_m \right\rangle\right) |n\rangle\langle m| \\ &\equiv \tilde{H}_e + \tilde{H}_{ph} + \tilde{H}_{e-ph}\end{aligned}, \tag{5}$$

where

$$\theta_n = \exp\left\{f_0 \sum_i g_{n,i}\left(b_i - b_i^\dagger\right)\right\}, \tag{6}$$

In this work, we focus on stationary electronic states and therefore on the new zeroth-order Hamiltonian $\tilde{H}_e$. The transformed Hamiltonian contains renormalized effective electronic coupling terms

$$\tilde{J}_{nm} = J_{nm} \left\langle \theta_n^\dagger \theta_m \right\rangle, \tag{7}$$

where the angle bracket $\langle\cdot\rangle$ denotes thermal average over the equilibrium phonon distribution. In the limit of f_0=0, $\left\langle \theta_n^\dagger \theta_m \right\rangle = 1$ and $\tilde{J}_{nm} = J_{nm}$, hence we recover the undressed exciton Hamiltonian in Eq. (1). In the limit of f_0=1, the effective coupling $\tilde{J}_{nm}$ is renormalized by an exponential factor, leading to fully dressed small-polaron states.

Varying f_0 allows full interpolation between the bare exciton description (the Redfield picture) to the fully dressed small-polaron description (the Förster picture) [38]. Therefore, the unitary transformation allows us to develop a unified theory that is applicable in the full parameter range of the exciton-phonon Hamiltonian.

To determine the optimal dressing factor, we apply Bogoliubov's theorem that yields the upper bound for the electronic Helmholtz free energy of the system:

$$A_0 = \frac{-1}{\beta} \ln \mathrm{Tr}\left\{ e^{-\beta \tilde{H}_e} \right\} \geq A_{exact} \tag{8}$$

Equation (8) provides us a means to determine the optimal dressing factor and therefore the optimal zeroth-order Hamiltonian at a given temperature and phonon spectral density by varying f_0 to minimize A_0. Note that the simple one-parameter variational ansatz used in this work lacks the flexibility to allow non-local phonon relaxation and could yield an unphysical abrupt transition in f_0 [38, 41-44]. This is not a problem in the parameter regime investigated here and therefore does not affect the conclusion of this work.

To demonstrate the dynamical localization effects predicted by the variational approach, we study the effective coupling of a dimer system whose spectral density has the following super-Ohmic form:

$$J(\omega) = \gamma_0 \frac{\omega^3}{\omega_c^2} e^{-\omega/\omega_c} \tag{9}$$

where ω_c is the cutoff frequency of the bath and γ_0 denotes the e-ph coupling strength. The reorganization energy of the spectral density, which is a measure of the e-ph coupling strength, is $\lambda=2\gamma_0\omega_c$. In Fig. 3, we plot the renormalized electronic coupling $J_{eff}=J_0\langle\theta_1^+\theta_2\rangle$ as a function of the inverse temperature (β) and γ_0 at $J_0=0.5\omega_c$ and $J_0=2\omega_c$. At high temperature and strong e-ph coupling, the renormalized electronic coupling decays to zero rapidly, signifying dynamical localization that destroys the coherence between the two chromophores in the dimer. More importantly, in the intermediate coupling regime, the renormalized electronic coupling that determines the steady-state electronic coherence is a complex function of J_0/ω_c, the temperature, the e-ph coupling strength, and the functional form of the spectral density. Since photosynthetic complexes often exhibit electronic couplings that are comparable to the reorganization energy of the e-ph couplings, the rich physics of the polaron problem and the spin-boson model should be considered, and the renormalization of the effective electronic coupling has to be taken into account in addressing the coherence effects in photosynthetic systems.

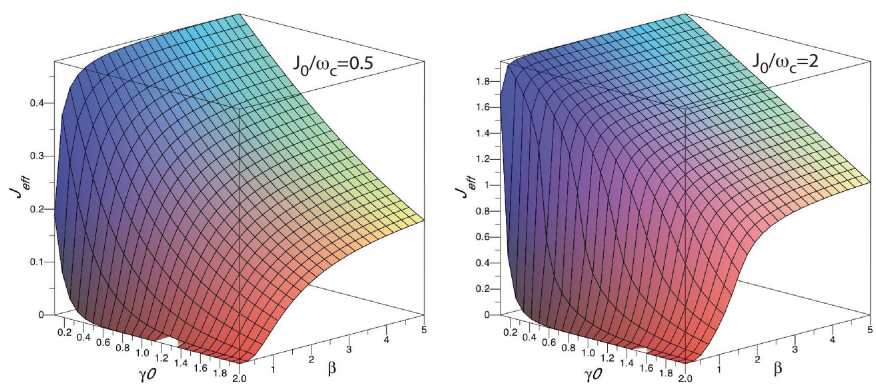

Fig.3. Renormalized effective electronic coupling as a function of e-ph coupling strength γ_0 and inverse temperature β at $J_0/\omega_c=0.5$ (left) and $J_0/\omega_c=2$ (right).

The magnitude of the bath reorganization energy is often compared with the value of electronic coupling as a criterion to determine the importance of coherence effects in photosynthetic EET. Therefore, it is instructive to investigate the temperature dependence of J_{eff} at constant bath reorganization energy and varying ω_c. Figure 4 plots

J_{eff} as a function of temperature for a model dimer with J_0=100 cm^{-1} and λ=50 cm^{-1} at different bath cutoff frequencies. The curves show that the renormalization of electronic couplings depends strongly on thermal population of phonon modes; therefore, the phonon frequencies contributing to the spectral density are also important to the nature of EET dynamics.

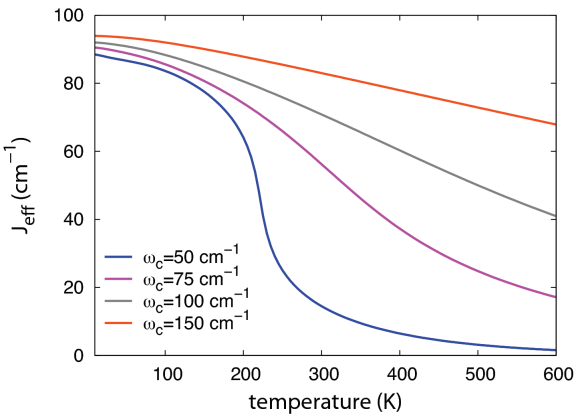

Fig. 4. J_{eff} as a function of temperature at various bath cutoff frequencies. The parameters are J_0=100 cm^{-1}, and the reorganization energy $\lambda=2\gamma_0\omega_c$=50 cm^{-1}. The parameters are typical for chromophores in photosynthetic complexes.

The results presented in this section indicate that for parameters typical for chromophores in photosynthetic complexes, the stationary states of photoexcitations are partially dressed and hence it is necessary to use a nonperturbative approach or a variational approach in order to describe the EET dynamics correctly. A potential scenario to verify this prediction is to investigate the lineshape of the B800 band at different temperatures to examine the temperature dependence of the coherence signature (Fig. 2). Indeed, the room-temperature absorption spectrum of the B800 band exhibits a less pronounced blue tail compared to the low-temperature spectrum, although the full description is complicated by the spectral density and temperature dependent distribution of the static disorder. A detailed investigation of the temperature-dependent B800 coherence based on the variational approach is currently a work in progress in our group.

5. Excitonic Coherence Generation via Intercomplex Transfer

The coherent wavelike motion of excitons observed in laser-induced dynamics in the B850 ring of the LH2 complex [34] and in recent two-dimensional electronic spectra of various photosynthetic complexes [6-9, 12] should not be taken for granted, because in natural photosynthesis, excitations in these complexes are generated either by the absorption of incoherent sunlight or by intercomplex EET from another photosynthetic complex. Though important to the implications of excitonic coherence effects, to what extent excitonic coherence can be generated in nature is still an open question that requires further investigation. In this Section, we examine the scenario of excitonic coherence generation via intercomplex EET.

Typically intercomplex EET is described either by the Förster theory or by the generalized MC-FRET theory [45, 46]. However, the MC-FRET picture considers energy transfer between excitonic eigenstates and therefore predicts no excitonic coherence generation during intercomplex EET. For instance, based on the MC-FRET theory, the B800→B850 EET does not generate excitonic coherence between B850 excitons, hence one might conclude that excitonic coherence, i.e. the wavelike motion of excitons, is not important in the B850 ring following the B800→B850 EET. Clearly, a discussion on the importance of the excitonic coherence effects in photosynthesis must go beyond the Förster picture of EET (which assumes no excitonic coherence) and address the generation of excitonic coherence in natural conditions.

We consider a model trimer system that is represented by the following exciton Hamiltonian:

$$H_e = \begin{pmatrix} E_1 & J_{12} & 0 \\ J_{12} & E_2 & J_{23} \\ 0 & J_{23} & E_3 \end{pmatrix}, \tag{10}$$

with $J_{12} \gg J_{23}$. The Hamiltonian represents a distant chromophore (site 3) coupled to a pair of strongly coupled chromophores (sites 1 and 2), and is a model for intercomplex transfer from site 3 to a coupled dimer. To include system-bath interactions, we also diagonally couple all three sites to independent baths described by the spectral density function for BChl Q_y excitations proposed by Jang and Silbey [47]. By assuming that the initial population is fully localized on site 3, we investigate the time-evolution of the reduced density of the system (ρ) using a non-Markovian time-nonlocal quantum master equation approach that was first proposed by Meier and Tannor [48, 49]. This method should yield reasonable results in this parameter regime.

Figure 6(a) presents the population dynamics in the site basis for a model system that is representative of a photosynthetic complex at 77 K. The results show a monotonic decay of ρ_{33}, which indicates incoherent dynamics as assumed in the MC-FRET theory. However, ρ_{22} and ρ_{11} clearly show reversible coherent dynamics in the anti-correlated population beats, which indicates that superposition between excitons (excitonic coherence) is generated within the strongly coupled dimer during the EET process. In contrast to the MC-FRET picture, our model predicts generation of excitonic coherence during the intercomplex EET process. To further investigate the coherence dynamics in the system, we compute the time-evolution of the concurrence, which is a measure of quantum entanglement and is defined as $C_{ij}=2|\rho_{ij}|$ [50], between all three pairs of chromophores. Figure 6(b) shows that superpositions between all three sites are dynamically generated and destroyed, resulting in complex coherence dynamics. Note that C_{12} denotes the coherence between the strongly coupled dimer, which eventually builds up to a large concurrence value because the lowest energy exciton in the system is delocalized on sites 1 and 2. Interestingly, C_{13} and C_{23} both reach a significant value before decaying at a later time, showing that although the population evolution does not indicate coherent dynamics, a significant amount of coherence between the weakly coupled donor and acceptor pair does appear in transient. Note that site 1 and site 3 are not directly coupled to each other; therefore, it is nonintuitive to see that C_{13} also reaches a significant value during the EET process. The result indicates that superposition between a distant pair of chromophores can be generated via a bridged, superexchange mechanism, even when one of the couplings is relatively small. Similar phenomena were also reported by Ishizaki and Fleming in their theoretical study of the FMO complex [14]. Note that in a more general picture coherences result in entanglements as described by M. Sarovar *et al.* [51].

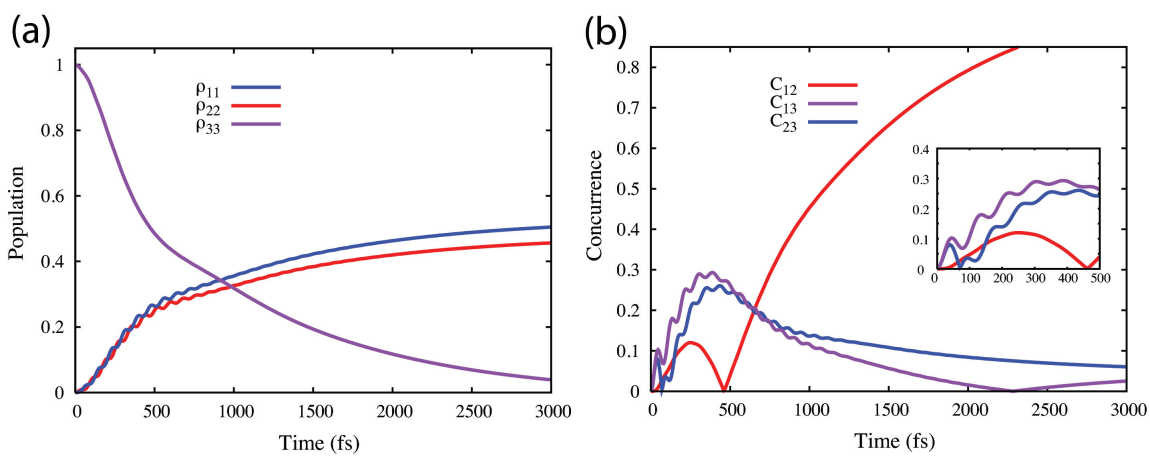

Fig.5. (a) Population dynamics in the site basis for a model trimer system with E_1=490 cm^{-1}, E_2=510 cm^{-1}, E_3=700 cm^{-1}, J_{12}=200 cm^{-1}, and J_{23}=20 cm^{-1}. The spectral density for the baths is the BChl spectral density function proposed by Jang and Silbey [47] with the γ_0 parameter set to 0.5 and the cutoff frequency set to 120 cm^{-1}. The temperature is set to 77K. (b) Time-evolution of the concurrences, defined as $C_{ij}=2|\rho_{ij}|$, for the same trimer system.

In summary, our model calculations demonstrate that in a seemingly incoherent intercomplex transfer process, quantum coherences between weakly coupled pairs and excitonic coherences between strongly coupled chromophores in the acceptor group can be generated. In other words, distant nonlocal quantum correlations can be generated in natural conditions that mimic intercomplex (or long-range) EET in light harvesting. These results are in agreement with recent theoretical calculations [14,51]. Furthermore, our model provides a plausible explanation for Scholes and coworkers' recent experimental observation that distant molecules within the photosynthetic proteins of marine algae are 'wired' together by quantum coherence [8].

6. Concluding Remarks

Quantum coherence plays fundamental roles in spectral tuning, energy storage, and EET dynamics of photosynthetic light harvesting, as demonstrated clearly in the LH2 antenna complex of purple bacteria. Our theoretical studies have provided much insight on exciton dynamical localization and excitonic coherence generation in photosynthetic systems. The variational-polaron approach indicates that decoherence of exciton states induced by dynamical fluctuations due to system-environment interactions, i.e. dynamical localization of excitons, is significant and cannot be avoided for a complete understanding of coherence and excitation dynamics in photosynthesis. In addition, our investigation into quantum coherence generation in intercomplex excitation energy transfer in natural photosynthesis shows that excitonic coherence between acceptor exciton states and transient nonlocal quantum correlation between distant pairs of chromophores can be generated through intercomplex energy transfer. The methods used in our theoretical studies go beyond conventional Redfield equation and Förster theory. In principle, the methods can be developed into new theoretical frameworks that will allow an adequate description of EET dynamics in photosynthesis, which is essential to the elucidation of the mechanisms and key components of quantum effects in photosynthetic light harvesting.

Acknowledgements

This work was supported by the National Science Council, Taiwan, under the Grant No. NSC98-2113-M-002-023-MY2. YCC also thanks National Taiwan University (College of Science and Center for Quantum Science and Engineering Subproject: 99R80870) for financial support.

References

[1] H. van Amerongen, L. Valkunas, R. van Grondelle, Photosynthetic Excitons, World Scientific Publishing Company, 2000.
[2] R.E. Blankenship, Molecular Mechanisms of Photosynthesis, Wiley-Blackwell, 2002.
[3] Y.-C. Cheng, G.R. Fleming, Annu. Rev. Phys. Chem. 60 (2009) 241.
[4] T. Renger, V. May, O. Kuhn, Phys. Rep. 343 (2001) 138.
[5] R. van Grondelle, V.I. Novoderezhkin, Phys. Chem. Chem. Phys. 8 (2006) 793.
[6] G.S. Engel, T.R. Calhoun, E.L. Read, T.-K. Ahn, T. Mancal, Y.-C. Cheng, R.E. Blankenship, G.R. Fleming, Nature 446 (2007) 782.
[7] H. Lee, Y.-C. Cheng, G.R. Fleming, Science 316 (2007) 1462.
[8] E. Collini, C.Y. Wong, K.E. Wilk, P.M.G. Curmi, P. Brumer, G.D. Scholes, Nature,463 (2010) 644.
[9] G. Panitchayangkoon, D. Hayes, K.A. Fransted, J.R. Caram, E. Harel, J. Wen, R.E. Blankenship, G.S. Engel, Proc. Natl. Acad. Sci. USA 107 (2010) 12766.
[10] M. Mohseni, P. Rebentrost, S. Lloyd, A. Aspuru-Guzik, J. Chem. Phys. 129 (2008) 174106.
[11] A. Olaya-Castro, C.F. Lee, F.F. Olsen, N.F. Johnson, Phys. Rev. B 78 (2008) 7.
[12] T.R. Calhoun, N.S. Ginsberg, G.S. Schlau-Cohen, Y.-C. Cheng, M. Ballottari, R. Bassi, G.R. Fleming, J. Phys. Chem. B 113 (2009) 16291.
[13] F. Caruso, A.W. Chin, A. Datta, S.F. Huelga, M.B. Plenio, J. Chem. Phys. 131 (2009) 105106.
[14] A. Ishizaki, G.R. Fleming, Proc. Natl. Acad. Sci. USA 106 (2009) 17255.
[15] H.-P. Breuer, F. Petruccione, The Theory of Open Quantum Systems, Oxford University Press, Oxford, 2002.
[16] T. Renger, R.A. Marcus, J. Chem. Phys.116 (2002) 9997.
[17] A. Ishizaki, G.R. Fleming, J. Chem. Phys. 130 (2009) 234111.
[18] Y. Yan, R.-X. Xu, Annu. Rev. Phys. Chem. 56 (2005) 187.
[19] B.P. Krueger, G.D. Scholes, G.R. Fleming, J. Phys. Chem. B 102 (1998) 5378.
[20] G.D. Scholes, I.R. Gould, R.J. Cogdell, G.R. Fleming, J. Phys. Chem. B 103 (1999) 2543.
[21] M. Chachisvilis, O. Kuhn, T. Pullerits, V. Sundstroem, J. Phys. Chem. B 101 (1997) 7275.
[22] V. Sundstroem, T. Pullerits, R. van Grondelle, J. Phys. Chem. B 103 (1999) 2327.

[23] X. Hu, T. Ritz, A. Damjanovic, F. Autenrieth, K. Schulten, Q. Rev. Biophys. 35 (2002) 1.
[24] H. Sumi, Chem. Rec.,1 (2002) 480.
[25] G.D. Scholes, G.R. Fleming, J. Phys. Chem. B 104 (2000) 1854.
[26] S. Jang, M.D. Newton, R.J. Silbey, Phys. Rev. Lett. 92 (2004) 218301.
[27] J. Struempfer, K. Schulten, J. Chem. Phys. 131 (2009) 225101.
[28] A. van Oijen, M. Ketelaars, J. Kohler, T. Aartsma, J. Schmidt, Biophys. J. 78 (2000) 1570.
[29] R. Agarwal, M. Yang, Q. Xu, G.R. Fleming, J. Phys. Chem. B 105 (2001) 1887.
[30] Y.-C. Cheng, R.J. Silbey, Phys. Rev. Lett. 96 (2006) 028103.
[31] S. Jang, M.D. Newton, R.J. Silbey, J. Phys. Chem. B 111 (2007) 6807.
[32] G.S. Schlau-Cohen, T.R. Calhoun, N.S. Ginsberg, E.L. Read, M. Ballottari, R. Bassi, R. van Grondelle, G.R. Fleming, J. Phys. Chem. B 113 (2009) 15352.
[33] O. Kuhn, V. Sundstroem, T. Pullerits, Chem. Phys. 275 (2002) 15.
[34] V.I. Novoderezhkin, D. Rutkauskas, R. van Grondelle, Biophys. J. 90 (2006) 2890.
[35] V. Novoderezhkin, M. Wendling, R. van Grondelle, J. Phys. Chem. B 107 (2003) 11534.
[36] K. Cho, Y. Toyozawa, J. Phys. Soc. Jpn. 30 (1971) 1555.
[37] E.I. Rashba, M.D. Sturge, *Excitons*, North-Holland, Amsterdam, 1982.
[38] D.R. Yarkony, R.J. Silbey, J. Chem. Phys. 67 (1977) 5818.
[39] T. Harris, R.J. Silbey, J. Chem. Phys. 83 (1985) 1069.
[40] R.J. Silbey, T. Harris, J. Chem. Phys. 80 (1984) 2615.
[41] Y.-C. Cheng, R.J. Silbey, J. Chem. Phys. 128 (2008) 114713.
[42] J. Allen, R.J. Silbey, Chem. Phys. 43 (1979) 341.
[43] A. Romero, D. Brown, K. Lindenberg, Phys. Rev. B 59 (1999) 13728.
[44] A. Romero, D. Brown, K. Lindenberg, J. Chem. Phys. 109 (1998) 6540.
[45] D. Beljonne, C. Curutchet, G.D. Scholes, R.J. Silbey, J. Phys. Chem. B 113 (2009) 6583.
[46] V.I. Novoderezhkin, R. van Grondelle, Phys. Chem. Chem. Phys. 12 (2010) 7352.
[47] S. Jang, R.J. Silbey, J. Chem. Phys. 118 (2003) 9324.
[48] C. Meier, D. Tannor, J. Chem. Phys. 111 (1999) 3365.
[49] Y.-C. Cheng, H. Lee, G.R. Fleming, J. Phys. Chem. A 111 (2007) 9499.
[50] W. Wootters, Phys. Rev. Lett., 80 (1998) 2245.
[51] M. Sarovar, A. Ishizaki, G.R. Fleming, K.B. Whaley, Nature Physics, 5 (2010) 1.